



HAL
open science

Mass transfer in emulsion polymerization: An experimental and modelling study

Estela Kamile Gelinski, Nida Sheibat-Othman, Timothy Mckenna

► To cite this version:

Estela Kamile Gelinski, Nida Sheibat-Othman, Timothy Mckenna. Mass transfer in emulsion polymerization: An experimental and modelling study. Canadian Journal of Chemical Engineering, inPress, 10.1002/cjce.25120 . hal-04275315

HAL Id: hal-04275315

<https://hal.science/hal-04275315>

Submitted on 8 Nov 2023

HAL is a multi-disciplinary open access archive for the deposit and dissemination of scientific research documents, whether they are published or not. The documents may come from teaching and research institutions in France or abroad, or from public or private research centers.

L'archive ouverte pluridisciplinaire **HAL**, est destinée au dépôt et à la diffusion de documents scientifiques de niveau recherche, publiés ou non, émanant des établissements d'enseignement et de recherche français ou étrangers, des laboratoires publics ou privés.

Mass Transfer in Emulsion Polymerization: an experimental and modelling study

Estela Kamile Gelinski¹, N. Sheibat-Othman^{2*}, T. F.L. McKenna^{1*}

¹ C2P2 UMR 5265, CNRS, CPE-Lyon, 43 Bd du 11 Novembre 1918, F-69616, Villeurbanne, France

E-mail: timothy.mckenna@univ-lyon1.fr

² LAGEPP UMR 5007, Université Claude Bernard Lyon 1, CNRS, 69622 Villeurbanne, France

E-mail: nida.othman@univ-lyon1.fr

ABSTRACT

A model is proposed to describe the impact of interphase monomer transfer on the emulsion polymerization of vinylidene fluoride (VDF). The model is validated with experimental data of the rate of polymerization and particle size distribution (PSD). During a typical emulsion polymerization process, the VDF monomer is in a gas or supercritical state, and thus much lighter than the aqueous phase in which the polymerization takes place. For this reason, the flux of monomer into the aqueous phase can depend on the type, number and distribution of agitators on the shaft, as well as the rotation rate. The new model incorporates the interphase mass transfer coefficient into a standard emulsion polymerization model to demonstrate the impact of the agitation (in the broadest sense) on the rate of polymerization and the PSD.

KEYWORDS

Emulsion polymerization, mass transfer, agitation, vinylidene fluoride, modelling

INTRODUCTION

As with many other chemical processes, the modelling of emulsion polymerization can be treated by levels of varying complexity. It is possible to use population balance methods to include any number of quality-related quantities including the particle size distribution (PSD), number of radicals in the particles, molecular weight and copolymer composition distributions. For instance, for the PSD, this approach allows us to account for different physical phenomena, including particle nucleation, growth, and coagulation. However, even if one wishes to use simpler approaches to calculate more basic information such as the rate of homopolymerization (R_p) with particles of identical size using equation (1), one thing remains common to all the models, namely the need to calculate the concentration of monomer in the polymerizing particles.

$$R_p = k_p [M]_p \frac{\bar{n} N_p}{N_A} \quad (1)$$

Where k_p is the rate constant for propagation, $[M]_p$ the monomer concentration in the particles, \bar{n} the average number of radicals per particle, N_p the number of particles per m^3 of latex, and N_A is Avogadro's number.

In an emulsion polymerization most of the polymer is produced inside the polymer particles. Monomer, present in the form of droplets in the early stages or as a separate feed phase in semi batch processes, must therefore be transferred through the continuous phase to the polymer particles. While it is theoretically possible for this to happen by diffusion, such mass transfer generally requires a sufficient level of agitation to increase the surface area between the phases, and proceed at a commercially viable rate. Despite the potential importance of agitation on emulsion polymerizations, it appears that very little academic research has been invested in this aspect of a widely studied process. It is often assumed that just so long as there is a sufficient level of agitation to assure decent heat transfer and homogeneity in the reactor, there is no need to consider this aspect any further. However, in certain instances, it is necessary to integrate the impact of agitation to fully understand what is taking place in the reactor. Table 1 presents the results of several studies on the influence of agitation rate (N) in emulsion polymerization found in the literature. This is not an exhaustive treatment of the subject, and we have voluntarily excluded studies in round bottomed flasks with agitation by magnetic stirring, and only included polymers made by conventional free radical mechanism.

If we consider the different systems with only liquid monomers, there are 2 major trends that appear. It is important to maintain a minimum rate of agitation to avoid phase separation of the droplets present during the initial stages of the polymerization. Without this, the monomers that are lighter than water tend to pool on the surface [1–6]. Beyond a certain point, increasing the intensity of agitation seems to provoke a drop in the polymerization rate, usually attributed to fewer particles. Fewer particles can be the result of high agitation rates causing monomer droplets to be more finely divided. This increases their surface area and thus uses surfactant for stabilization of the droplets that could otherwise be used to nucleate particles. [4,5] Also higher agitation can provoke the orthokinetic coagulation of the particles. [1,3,7–11] Finally, in studies where highly insoluble species are present, increasing the agitation rate can have different kinetic effects. In the case of an emulsion polymerization in the presence of highly insoluble dodecyl mercaptan (DDM) as a chain transfer agent (CTA), increasing the agitation rate increases the rate of mass transfer of the DDM to the particles. The results show no impact on the observed R_p , but a reduction in the average molecular weight. [5,12] In one of these studies, an effect was seen only when passing from 70 to 150 rpm, but no change in the average molecular weight was observed beyond 150 rpm. [5] This underlines the fact that the design and geometry of the reactor and the agitation system can be quite important, and that it is necessary to be cautious when drawing conclusions on agitation from a single paper. Similar effects were seen in cases where very sparingly soluble monomer such as butyl methacrylate was used, [6] or when studying the impact of inhibitors such as dissolved oxygen. [13,14] The authors of reference [14] proposed a process model based on the use of gas-liquid mass transfer coefficient ($k_L a$, see below) to account for the increased inhibition by oxygen and induction period seen at higher agitation rates.

Table 1. Impact of agitation on emulsion polymerizations (L = liquid, V = vapour, SC = supercritical)

Monomer (Phase)	Reactor Operation	Observations	Ref.
Systems with liquid monomers			
Styrene (Liquid, L)	<ul style="list-style-type: none"> • 0.3 and 1.3 L round-bottomed glass reactors. • 50 °C. 	<ul style="list-style-type: none"> • R_p decreases when increasing agitation rate from 410 to 1050 rpm. • N_p decreases as N increases, due to coagulation at higher rpm. 	[7]
Styrene (L)	<ul style="list-style-type: none"> • 0.75 L jacketed glass reactor. • Stainless steel stirrer, with anchor at the bottom and 3 impellers with 2 pitched (45°) blades at right angles. • Polymerization in presence of dodecyl mercaptan (insoluble in water). 	<ul style="list-style-type: none"> • No influence of N on R_p. • Increasing N from 200 to 275 then 350 rpm decreases the molecular weight (M_w) by improving mass transfer of highly insoluble CTA. 	[12]
Styrene (L)	<ul style="list-style-type: none"> • Cylindrical round-bottomed glass reactor with 4 baffles and anchor or half-moon agitators. • Batch polymerizations at 70 °C. • Polymerizations at 150, 200, 300 and 400 rpm. 	<ul style="list-style-type: none"> • With anchor, if N too low (150 rpm) we get phase separation and low reaction rate. • Highest R_p with anchor observed at 200 rpm. • Above 200 rpm, N_p drops as N increases, slowing the rate. 	[1]
Styrene (L)	<ul style="list-style-type: none"> • 2 stainless steel reactors of 1.85 and 7.48 L, each equipped with geometrically similar six blade Rushton turbines (radial flow), or with a pitched (45°) six blade impeller (axial flow). • 4 baffles inserted in the reactors. 	<ul style="list-style-type: none"> • Some minimum level of dispersion is needed to avoid mass transfer limitations due to droplet coalescence. • This will depend on vessel size, monomer content and impeller type. • R_p increased with N from 250 to 360 rpm, and particle diameter (d_p) decreased. • Beyond 360 rpm little change was noticed. • Scale-up with Rushton turbine is the best at constant tip speed, for pitched blade at constant energy dissipation. 	[2]
Styrene (L)	<ul style="list-style-type: none"> • 1 L glass reactor operated in batch mode with a paddle agitator. • Polymerization at 50 °C. 	<ul style="list-style-type: none"> • No observable coagulation and both conversion and M_w increase as N increases. • d_p does not change, suggesting some sort of mass transfer limitation due to agitation. 	[15]
Methyl-methacrylate (L)	<ul style="list-style-type: none"> • 2 L batch reactor with different agitation setups: single and double pitched blade turbine, single and double Rushton turbine. • Polymerizations at 50-60 °C. 	<ul style="list-style-type: none"> • R_p increases from 20 to 250 rpm, then coagulation of particles results in a decrease upon increase to 350 rpm. • Foaming observed at 350 rpm. 	[3,8,9]

		<ul style="list-style-type: none"> • Adding baffles causes drop in R_p at 250 rpm, but a higher M_w. • Addition of a second impeller leads to slightly higher R_p at same N 	
Methyl-methacrylate (L)	<ul style="list-style-type: none"> • Flat bottomed reactor with 4 baffles and a Rushton turbine (not clear how many blades). • Soapless polymerization in a 10 L semi-batch stirred tank reactor operated at 65 °C. • 2 feed types: one more, one less hydrosoluble. • Agitation rate from 200 to 500 rpm. 	<ul style="list-style-type: none"> • A minimum agitation rate is needed to sufficiently disperse monomer droplets. • In the presence of droplets, initial R_p and M_w are higher at low stirring speeds. • No impact of stirring on seeded polymerization (similar M_w, N_p and R_p). 	[4]
Vinyl Acetate (L)	<ul style="list-style-type: none"> • 2 L jacketed glass CSTR with paddle agitator. • N varied from 320 to 560 rpm. 	<ul style="list-style-type: none"> • Like in Krishnan et al., high agitation rates led to long induction times and lower R_p due to enhanced oxygen inhibition. 	[13]
Styrene (L) + Copolymerization with non-specified monomers (L)	<ul style="list-style-type: none"> • 2 L jacketed semi-batch reactor. • Stirrer non-specified, N from 100 to 200 rpm. 	<ul style="list-style-type: none"> • Nucleation is independent of N. • $N = 180$ rpm leads to coalescence. • $N = 220$ rpm leads to foaming. 	[10]
Styrene (L) + Butyl Acrylate (L)	<ul style="list-style-type: none"> • 2 L semi-batch reactor with an anchor stirrer (diameter or anchor = 0.75 diameter of reactor). • N varied from 70 to 220 rpm. 	<ul style="list-style-type: none"> • Increasing N from 70 to 150 rpm increases R_p (no coagulation), but there appears to be no effect on N_p. R_p is limited by mass transfer of monomer from droplets at low N. • Increasing N from 150 to 220 rpm does nothing. • Increase of N from 70 to 150 rpm increases M_w in the absence of dodecyl mercaptan (DDM) because of enhanced mass transfer to the particles. Increasing N from 150 to 220 rpm does nothing. • Preemulsifying the feed (see Kemmere et al.) attenuates (but does not eliminate) these effects. • In the presence of DDM the impact of agitation on R_p does not change, but M_w continually decreases as N increases due to enhanced mass transfer of the DDM. 	[5]
n-butyl methacrylate (BMA)-N-methylol acrylamide (NMA) (both L)	<ul style="list-style-type: none"> • Polymerization in 2 L glass reactor with 6 baffles. • 2 different agitators: A310 (fluidfoil, 3 pitched blades, axial flow) or a Rushton Turbine (radial flow). • Agitator diameters 4, 6, 8 cm. • Focused on formation of coagulum. 	<ul style="list-style-type: none"> • NMA is highly water soluble so agitation can increase its incorporation in the particles. • Agitation will also impact R_p through enhanced mass transfer of highly insoluble butyl methacrylate through water by increasing the surface area of the droplets. • Noticed phase separation of BMA for small agitator and low N, otherwise appears to be only small difference in R_p. 	[6]

		<ul style="list-style-type: none"> • N_p decreases as N increases for all impellers, greater effect for larger impellers. • Coagulation increases with time, with N, with impeller size, and is more important for radial flow than axial flow because of the trailing vortex. 	
n-Butyl Methacrylate (L)	<ul style="list-style-type: none"> • Polymerization in a 1 L jacketed RC1 calorimeter. • Agitator 6 blade Rushton turbine with N varied from 300 - 800 rpm. • Study run to look at mass transfer of oxygen during polymerization. 	<ul style="list-style-type: none"> • Phase separation noted for $N < 300$ rpm. • Ran with low surfactant and low solids. • Induction periods seen to increase as N increases when oxygen present (no induction noted with no oxygen in reactor). Attribution to enhanced gas-liquid mass transfer at high N. • Increasing N in presence of oxygen led to an increase in N_p from $\sim 7.0 \times 10^{16}$ at 300 rpm to $\sim 9.8 \times 10^{16}$ at 800 rpm • Propose a model based on gas-liquid mass transfer to explain the effect of oxygen. 	[14]
Butyl Acrylate (L)	<ul style="list-style-type: none"> • Surfactant-free semi-batch polymerization in a 1 L glass reactor with a 4-bladed agitator at 80 °C. • Total solids content up to 40 %. 	<ul style="list-style-type: none"> • Significant coagulation as N increased from 400 to 800 rpm. The authors estimate there is no coagulation at 400 rpm. • Lower yields at higher N, probably linked to lower N_p. 	[11]
Vinyl Acetate (L)	<ul style="list-style-type: none"> • Glass batch reactor with Teflon stirrer, and agitation rates of 75, 150 and 220 rpm. • Polymerization at 60°C. 	<ul style="list-style-type: none"> • Phase separation at 75 rpm. • R_p increases with increasing N. 	[16]
Systems with at least one gaseous monomer			
Ethylene (Vapor, V) + Vinyl Acetate (L)	<ul style="list-style-type: none"> • Semi-batch polymerization in 2 L reactor with ethylene introduction through a sparger, and a height to diameter ratio (H/D) of 2.6. • Pitched blade and Rushton turbines with N between 200 and 400 rpm. 	<ul style="list-style-type: none"> • Importance of mixing because of the presence of the vapor phase ethylene. • A high H/D is important to enhance contact time between gas and colloids, and vortex formation is a useful feature with the gaseous monomer to enhance mass transfer. • Use of a porous sparger led to more foaming than introduction of ethylene through point source. • At 400 rpm could not sample because of foaming. • Increasing N enhances ethylene concentration and leads to lower rate of vinyl acetate consumption because it polymerizes more slowly. 	[17]

		<ul style="list-style-type: none"> • Combination of agitators and N allows one to reach point where ethylene mass transfer is no longer limited by the mixing. 	
Ethylene (V) + Vinyl Acetate (L)	<ul style="list-style-type: none"> • Polymerization in a 1.8 L semi-batch RC1 calorimeter with a stainless steel anchor agitator operated at 200 to 300 rpm. • Pressure up to 30 bar and reactor temperature between 65-80 °C. 	<ul style="list-style-type: none"> • Increasing N increased ethylene dissolution rate and thus R_p. This also has an impact on the copolymer composition. • Decrease in mass transfer rate as viscosity (solids content) increases. 	[18]
Ethylene (V) + Vinyl Acetate (L)	<ul style="list-style-type: none"> • Batch emulsion polymerization in a 7.5 L stainless steel reactor. • Agitation rate from 200 to 500 rpm (agitator not clearly specified). 	<ul style="list-style-type: none"> • Ethylene content in the copolymer increases as N is increased from 250 to 450 rpm due to greater ethylene solubilization (mass transfer). 	[19]
Ethylene (V), vinyl acetate (L), N-methylol acrylamide (L)	<ul style="list-style-type: none"> • 18 L stainless steel semi-batch reactor with 2 baffles and a Rushton turbine. • Pressure not specified, T between 55 and 80 °C. 	<ul style="list-style-type: none"> • Increasing N increases d_p due to coagulation. 	[20]
Tetrafluoroethylene (V)	<ul style="list-style-type: none"> • 1 L reactor with anchor impeller and a baffle plate. • N varies from 250-750 rpm. • $P = 4$ bars and $T = 75$ °C ($P_c = 38.9$ bars, $T_c = 33$ °C [21], so monomer is vapor). 	<ul style="list-style-type: none"> • Chose the anchor agitator because it gave a good vortex and a baffle inserted to enhance turbulence. • Solubility of TFE very low, measured at 0.002 mol/L at reaction conditions. • For N between 250 and 500 rpm, R_p increases quickly then levels off, with the plateau being higher as N increases. At 750 rpm, get rapid activation, followed by rapid drop in R_p (i.e. coagulation of particles). • Type of baffle and agitator are very to enhance contact between particles and gas. 	[22]
Vinyl Chloride (V)	<ul style="list-style-type: none"> • 5 L stainless steel reactor with either a 3-blade propeller or an anchor agitator. • Reactor temperature 55 °C and pressure adjusted to be 97 % of saturation pressure. 	<ul style="list-style-type: none"> • R_p and M_w both increase noticeably from 500 to 1000 rpm. Mass transfer limitations at low N, but that no longer exist after 1000 rpm. • At low N, the anchor agitator seems to be more effective in incorporating the gaseous monomer, and mass transfer limitations disappear around 600 rpm. 	[23]
Vinylidene fluoride (Supercritical, SC)	<ul style="list-style-type: none"> • 4 L reactor with 4 impellers (either 4 pitched blade impellers with 4 blades at 45°, or 1 hydrofoil plus 3 pitched blades). • Temperature 88 °C, pressure 83 bars (constant in semi-batch, initial in batch). • N from 350 to 650 rpm in batch and semi-batch mode. 	<ul style="list-style-type: none"> • Increasing N increases R_p and M_w, especially when using the hydrofoil. • No significant coagulation and final N_p is independent of N. • Rate of polymerization was directly correlated with gas-liquid mass transfer coefficient $k_{L,a}$. 	[24]

<p>Vinylidene fluoride (V), Hexafluoropropylene (V)</p>	<ul style="list-style-type: none"> • Semi-batch polymerization in a 10 L reactor with 2 variable width baffles and 1 three-blade turbines. • Reactor temperature 85 °C, total pressure less than 40 bars so both components in vapor phase. • Surfactant free polymerization. 	<ul style="list-style-type: none"> • Reference N is 550 rpm. Although not shown in the publication, the authors state that the agitation conditions must be chosen to avoid mass transfer limitations that occur at $N < 550$ rpm. 	<p>[25]</p>
<p>Chlorotrifluoroethylene (V), vinyl acetate (L), butyl acrylate (L), Veova 10 (L)</p>	<ul style="list-style-type: none"> • Batch emulsion polymerization at 60 °C in stirred autoclave. No other information given. 	<ul style="list-style-type: none"> • Increasing N increases dissolution of the chlorotrifluoroethylene in the liquid phase, and thus increases monomer consumption and generates larger particles. 	<p>[26]</p>

In systems with gaseous (V) (or supercritical, SC) monomers, the monomers are typically quite insoluble in water, and given the fact that they are significantly lighter than water, mechanical agitation and good reactor design are important in maintaining sufficient concentrations in the aqueous phase or polymer particles. For instance, reactor height to diameter ratios higher than normal ($H/T > 1.5$ [27]) can help enhance the contact time between the bubbles of monomer and the continuous phase, thereby increasing monomer availability in the particles. [17,24,28] Scott et al. [17] suggested that using gas spargers in the bottom of the reactor can help as well, but these can lead to increased foaming if care is not taken. However, just like with the dissolved oxygen in reference [14], studies with ethylene [17–20], vinyl chloride in the vapor phase [23], and fluorinated monomers [22,24–26,28] all showed that increasing the agitation rate (regardless of the shape of the reactor and type of agitator) led to a measurable increase in the rate of polymerization (and molecular weight [24]). Once again, the magnitude of the changes will depend on the design of the reactor and agitator [22,24].

If we consider a system with a supercritical or gaseous monomer, where the monomer is much lighter than the continuous phase, mechanical agitation of the reactor will be designed to entrain the gas in the head space of the reactor into the liquid where it will be dispersed in the form of bubbles. The flux of monomer from the bubbles into the continuous aqueous phase of the reactor will be governed by the following equation:

$$V_w \frac{dA_1}{dt} = k_L a V_w (A^* - A_1) - r V_w - Q_L A_1 \quad (2)$$

where V_w is the volume of water in the reactor, A_1 the concentration of component A in the water, t the time, k_L the liquid mass transfer coefficient, a the gas-liquid interfacial area per unit of volume of the dispersion, A^* the equilibrium concentration of A in the liquid, r the reaction rate per unit volume and Q_L is the exit flow rate of liquid phase (equal to zero in batch and semi-batch operations). The equilibrium concentration A^* is a thermodynamic property (and can be approximated using for instance Henry's law) affected only by pressure and temperature, not by fluid dynamics or mixing. The concentration of A in the liquid (A_1) is affected by the transport and reaction rate.

One of the challenges in solving this equation is to estimate the value of the product $k_L a$ (it is very difficult to estimate the values separately). While it would be desirable to be able to estimate $k_L a$ a priori, Krishnan et al. [14] used this method to estimate the impact of changing levels of dissolved oxygen on the rate of polymerization, and in particular the induction period for the emulsion polymerization of n-butyl methacrylate (BMA). While the method showed reasonable results, a good fit to the experimental data required that they use adjustable parameters in their model. As they pointed out, one of the problems is that they used correlations for $k_L a$, and many of the available correlations can show errors of $\pm 50\%$ in these situations as they are a function of many system dependent variables as noted above. As an example of what this means, Chaudhari et al. [29] compared $k_L a$ values for a dead-end reactor using different methods: dynamic physical absorption, catalytic hydrogenation of styrene and oxidation of sodium sulfite. From the results, it was possible to state that the different methods led to a similar mass transfer coefficient and that the mode of introduction of gas in the system also influences the coefficient. However, when a dip tube was used to introduce the gas, the $k_L a$ values increased in 3 to 5 times in a manner not accounted for by any correlations. For this reason, experimental methods are often used to estimate the value of this product. One commonly used means of estimating this values is the dynamic pressure method [29–31], which consists in monitoring the pressure drop caused by the absorption of gas A in the

liquid over time. In the absence of reaction, the concentration of the gas A in the liquid is related to the pressure drop in the reactor as follows:

$$V_w \frac{dA_l}{dt} = - \frac{V_g}{RT} \frac{dP}{dt} \quad (3)$$

where V_g is the volume of gas in the reactor, P the pressure, Z is the compressibility factor, R the gas constant and T is the temperature. Mendez Ecosia et al. [24] used this method to estimate $k_L a$ for the reactor used in our current study and showed that it was a very strong function of the agitation rate.

This review shows that automatically neglecting *a priori* mass transfer in emulsion polymerization can lead to a poor choice of operating conditions, where mixing can have an impact on polymer properties and the polymerization rate. This is especially true when dealing with highly insoluble reactive species, be they monomers or impurities. Some studies have shown that using a $k_L a$ -based approach can account for the non-equilibrium partitioning of light gaseous or supercritical reactants, such as vinylidene fluoride (VDF) which is the object of the current paper. It appears necessary to use an experimental approach to estimate $k_L a$ rather than to use existing correlations as these do not account for the true nature of all types of agitators or reactor geometries, nor for changes in viscosity due to the accumulation of polymer in a semi-batch system. [17] For these reasons, we propose a simplified model of the emulsion polymerization of VDF under supercritical conditions that will allow us to account for the impact of mass transfer in a manner similar to that of Krishnan et al. [14]. The model is compared to experimental data, and it is shown that if one has a good estimate of $k_L a$ it is possible to accurately model the impact of stirring on the polymerization rate and particle size distribution under conditions where the number of particles in the latex is known (i.e. once particle nucleation is finished and coagulation is assumed negligible).

MATERIALS AND METHODS

Polymerization

The high pressure reactor used for polymerization in this study is a 3.8 L stainless steel 316 jacketed reactor with three 6-bladed 45° impellers of 5 cm diameter and one hydrofoil of 9.1 cm diameter, a dip tube and a thermocouple located 5 mm from the reactor wall. The reaction is performed with an initial charge of 1.6 liters of water and the following composition,

Surfactant (g/L)	1.50
Paraffin (g/L)	3.70
Chain Transfer Agent (g/L)	13.50
Initiator (g/L)	0.15
Buffer (g/L)	0.10
Monomer (g/L)	562

The monomer is added by activating the pump manually when the reactor pressure is 0.5 bar below the set-point. The polymerization rate is calculated by calorimetry from data recorded each 10 seconds. The reactor geometry and internals disposition, as well as more details on the experimental mode of operation for semi-batch polymerization are presented elsewhere [24]. The dimensions and arrangement of the impellers are shown in

Figure 1. The reactor has a height to diameter (H/T) of 5 and the height of the conical section (h_c) is 3 cm. The position of the impellers in the agitation setup can be changed, and in this work two setups are used:

- Setup 2: three 6-bladed 45° impellers plus hydrofoil A345 (pumping up).
- Setup 2D: three 6-bladed 45° impellers plus hydrofoil A315 (pumping down).

The difference between the two can be seen in Figure 2.

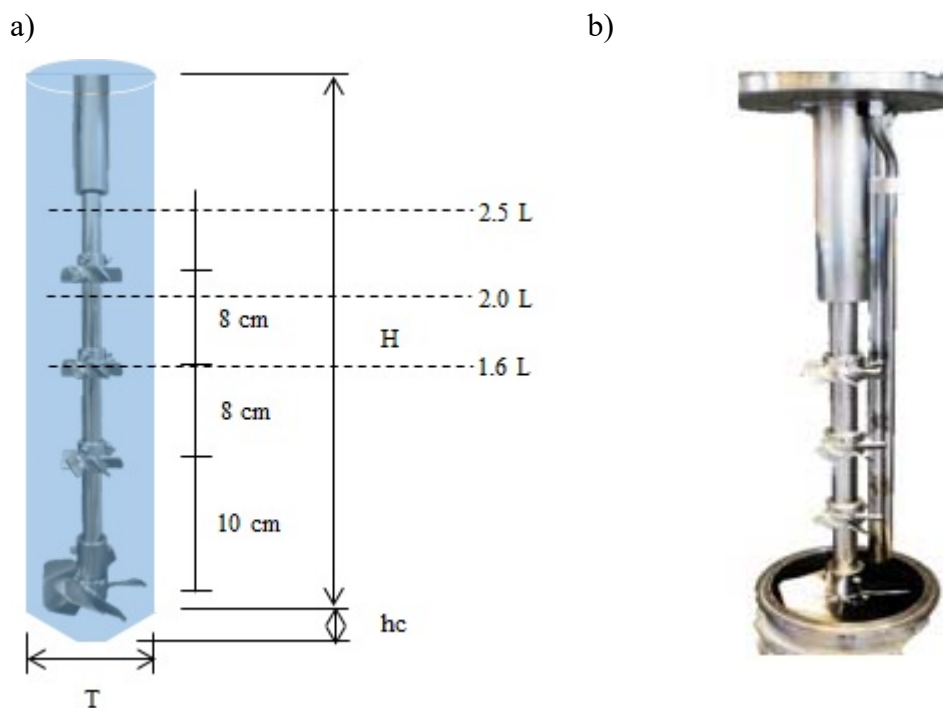


Figure 1: a) Reactor geometry, impellers spacing for Setup 2/2D and volumes, b) Reactor internals showing the thermocouple and dip tube.

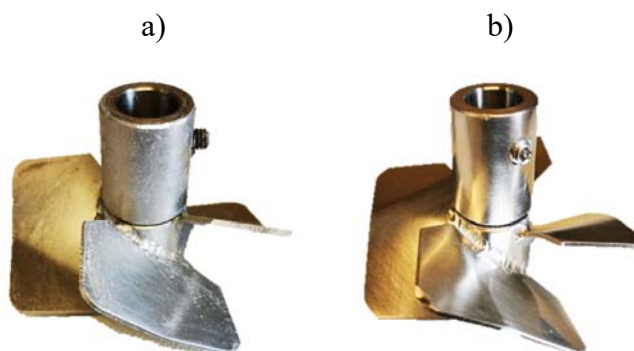


Figure 2: Hydrofoil in the a) A345 (setup 2, pumping up), and b) A315 (setup 2D, pumping down) configurations.

The vinylidene fluoride (VDF) monomer and proprietary surfactant (TA) were kindly provided by Arkema (Pierre Bénite, France), and used without further purification. Potassium Persulfate (KPS) (99 %, Acros Organics) was used as initiator, Ethyl Acetate (99.5 %, Sigma Aldrich) was used as chain transfer agent (CTA) and Sodium Acetate Anhydrous (Salt) (99 %, Sigma Aldrich) was used as a buffer. Deionized water is used as

initial charge, as rinse water and to prepare the initiator and salt solution and a commercial paraffin/wax is used as antifouling agent. The semi-batch emulsion polymerization is performed with a surfactant concentration below its critical micellar concentration, so the particles are created by homogeneous nucleation. The reaction is performed at 83 °C and 88 bar (so under supercritical conditions of VDF, $P_c = 44.3$ bar and $T_c = 30^\circ\text{C}$), using the setup 2 or setup 2D at 400 or 550 rpm as described in [24].

The solids content (SC) is measured by gravimetry, and the particle diameter (d_p) is measured using the Zetasizer®, so the number of particles (N_p) can be calculated. The surface coverage (θ) is calculated based on the parking area of the surfactant, 25 \AA^2 . [24] The Size Exclusion Chromatography (SEC) technique is used to measure the molecular weight (M_w) of the samples, using DMSO as solvent.

Semi-batch reactions were performed with the two different setups and agitation speeds for 120 minutes and the polymerization curves are shown in Figure 3. It is possible to observe that there is no significant difference in the reaction rate for the two setups when the speed is 550 rpm. There seems to be an optimal agitation configuration for which the mass transfer limitations are no longer acting, which is the case for 550 rpm with setup 2 and setup 2D.

As expected from the previous literature, the polymerization rate is slower for a lower agitation speed, as the mass transfer coefficients are in average 75 % lower than the values found for 550 rpm. It is interesting to observe that during the period 0 to 40 min, where the level of the latex and its viscosity are still low, so ensuring a good quality of mixing, the three curves are very similar (also leading to similar N_p , see Table 2).

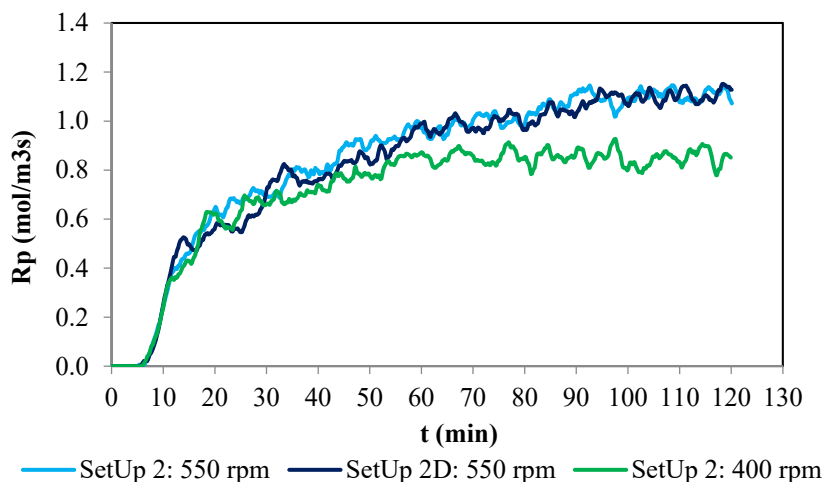


Figure 3: Semi-batch polymerization rates of reactions performed with different setups and speeds.

The results of these reactions are presented in Table 2. The consequence of working with higher mass transfer coefficients (see below) is seen in the increase in the solids content (SC) and in the weight average polymer molecular weight (M_w), especially when comparing the reactions performed with the same setup at different speeds. In the table, N_p refers to the number of particles per unit volume, PdI is the polydispersity index of the particle size, PDI is the polydispersity index of the molecular weight, and θ is the surface coverage by the surfactant.

Table 2 Semi-batch polymerizations performed with different setups and speeds.

	Setup 2 400 rpm	Setup 2 550 rpm	Setup 2D 550 rpm
Time (min)		120	
SC (%)	29.4	34.6	35.8
d_p (nm)	208	221	225
PdI	0.012	0.021	0.007
$N_p \times 10^{-19}$ (m⁻³)	4.3	4.3	4.3
θ (%)	8.0	7.0	6.9
M_w (kDa)	398	457	485
PDI	2.51	2.37	2.50

Estimation of $k_L a$

The experiments to determine $k_L a$ are based on the dynamic physical absorption method proposed by Chaudhari et al. [29] which consists in monitoring the pressure drop caused by the absorption of a gas A in a liquid over time, and were performed as indicated by Mendez Ecoscia et al. [24]. The reactor was charged with a latex 10 wt % kindly provided by Arkema and the experiments were performed at the same temperature used to run the reactions. As the pressure drop in our system is reliable when performing the experiments below 40 bars, the experiments were performed at 30 bars, and we will assume that the pressure will not significantly impact the estimate of $k_L a$. Obviously changing the pressure will impact the density of the gaseous or supercritical fluid and thus the specific surface area a (more particularly for VDF, the fluid is supercritical at 88 bar and 83 °C, but not at 30 bars). However, the work of Teramoto et al. [32] on the estimation of several process gases suggests that the variation of $k_L a$ is negligible over variations of pressures from 10 to 100 atm.

The experiments were performed for setups 2 and 2D and the results are presented in the Table 3. In most cases, setup 2D has a higher $k_L a$ value. Also, it is clear that the values at 400 rpm are lower than for 550 rpm, and thus not sufficient to maintain a full rate control of the polymerization. Note that in Figure 3 the initial latex volume was approximately 1.7 L (very close to the 2nd impeller, thus ensuring a good mixing), so no difference on R_p was observed between both setups at 550 rpm.

Table 3 $k_L a$ estimation results for Setups 2 and 2D for different volumes and speeds.

V_w (L)	N (rpm)	$k_L a$ (min ⁻¹)	
		Setup 2	Setup 2D
2.0	400	1.109	0.727
	550	2.681	2.876
2.5	400	0.386	0.505
	550	1.320	1.705

The mass transfer coefficient can be estimated by the following equation, adapted from the work of Chaudhari et al. [29],

$$k_L a = A \left(\frac{V_g}{V_w} \right)^B N^C \quad (4)$$

where $k_L a$ is the mass transfer coefficient in min^{-1} , V_g is the volume of gas or headspace available in the reactor in m^3 , V_w is the volume of liquid in m^3 and N is the agitation speed in rpm. The constants for setup 2 (400 and 550 rpm) and setup 2D (550 rpm) are given in Table 4.

Table 4 Coefficients for $k_L a$ estimation.

	A	B	C
Setup 2	2.57×10^{-8}	1.369	2.95
Setup 2D	0.869	1.040	0.207

Even knowing that the original equation from Chaudhari et al. [29] was obtained for a dead-end autoclave reactor with a single impeller, the estimated values we found with our correlations, are pretty close to the experimental ones as shown in Figure 4.

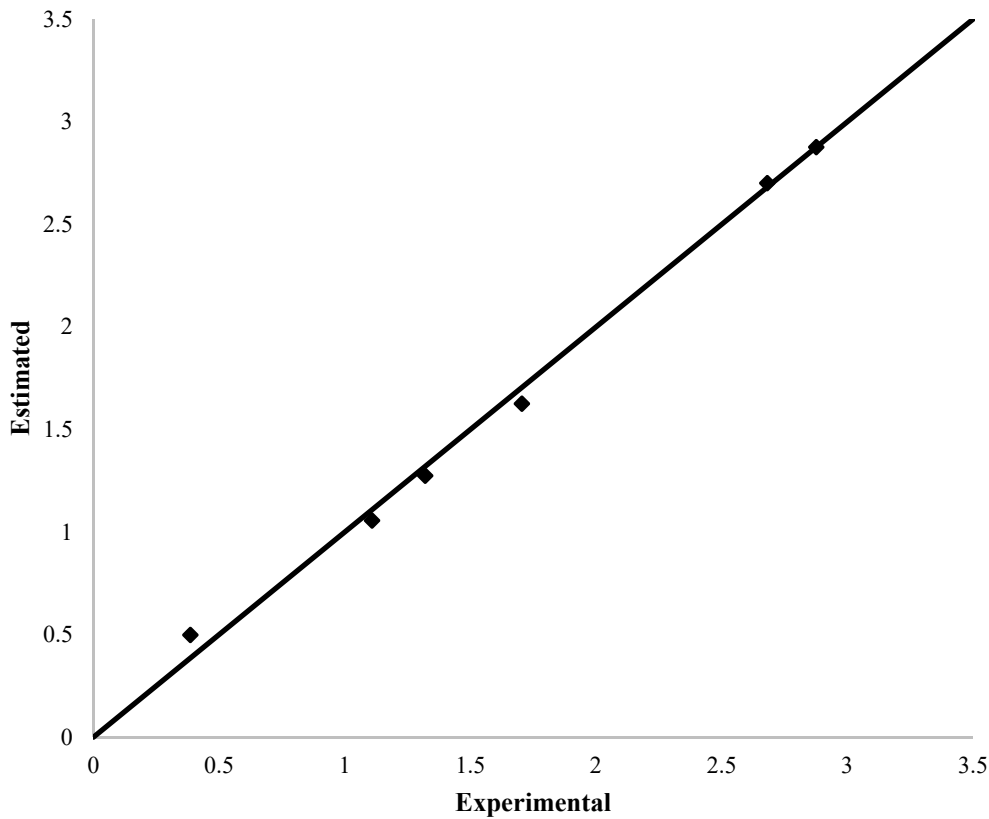


Figure 4 Estimated-Experimental $k_L a$ values (min^{-1}).

MODELLING EMULSION POLYMERIZATION

The rate of polymerization for the process carried out as an emulsion is given by equation (1). The emulsion polymerization model is based on the works and reactions constants of Apostolo et al. [25] and Pladis et al. [33,34]. The current version of this model does not

take into consideration the nucleation and coagulation of particles, thus modelling only the growth of particles.

The partial differential equation representing the PSD was discretized to become a set of ordinary differential equations, using finite differences on diameters, and solved using Matlab®. The fitting parameters to the model can be: the efficiency of radical absorption (f_e , here taken equal to 1), the desorption coefficient (the model is taken from [34], but the parameters refitted) and the choice among different models for radical entry/exit (two exit models were compared). Note that the desorption coefficient is valid only for the considered operating conditions (i.e. concentration of CTA, temperature, particle size), and in order to make it valid for a wider range of operation more experiments and a more detailed model would be required.

Kinetics, mass balances and PSD

The free radical homopolymerization scheme taken into consideration as well as the material balance equations are presented below and the material balances are given in Table 5. We assume equi-partitioning of CTA between particles and water. Note that the PVDF produced by emulsion polymerization is semi-crystalline. Also, during the polymerization of VDF, the mobility of the hydrogen atoms of VDF is responsible for the chain transfer to monomer and to polymer (backbiting) reactions and bimolecular termination by disproportionation. While this influences the polymer molecular weight distribution, it has a minor effect on the reaction rate and therefore was not considered in the kinetic scheme where we are focusing only on predicting the rate of reaction. Finally, a better description of D_p would be needed for a better description of the polymerization.

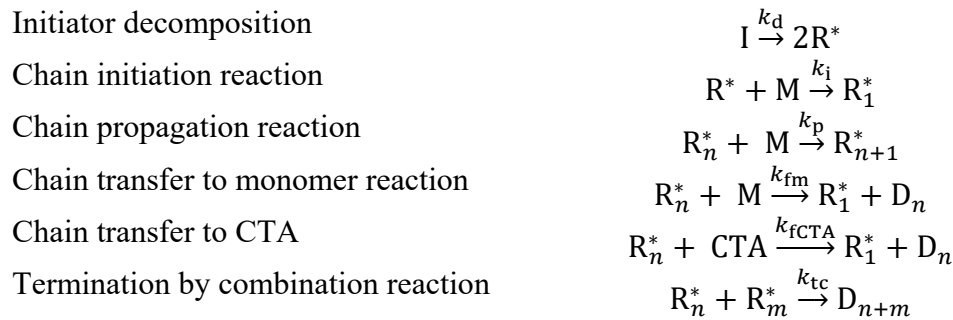


Table 5. Model for emulsion polymerization. [35–38]

Mass balances	
Initiator	$\frac{d[I]}{dt} = -k_d[I]$
Oligomeric radicals in the aqueous phase (length 1 to j_{cr})	$\frac{d[R^*]_w}{dt} = 2f_1k_d[I] - \frac{[R^*]_w V_e}{N_A V_w} \int_0^\infty k_e(v)f(v)dv - k_{tw}[R^*]_w^2 + \frac{1}{N_A} \frac{V_e}{V_w} \int_0^\infty k_{des}\bar{n}(v,t)f(v)dv$
Reaction rate in particles (mole $s^{-1} m^3$ emulsion)	$R_p = (k_{tm} + k_p) \frac{[M]_{p,am}}{N_A} \int_0^\infty \bar{n}(v,t)f(v)dv$
Volume of the swollen particle phase	$V_{part} = V_p + V_m^p = V_p \frac{1}{(1-[M]_p) \frac{M_{w,m}}{\rho_m}}$
Volume of the unswollen polymer phase	$\frac{dV_p}{dt} = \frac{M_{w,m}}{\rho_p} R_p V_e$

Volume of the emulsion (water, polymer and dissolved monomer)	$V_e = V_{\text{part}} + V_w + V_m^w$, with $V_m^w = \frac{[M]_w M_{w,m} V_w}{\rho_m}$
Number of particles in the reactor per unit volume	$N_p = \int_0^\infty f(v, t) dv$
Radical entry into particles	
Frequency of radical entry	$\rho = k_e [R^*]_w$
Diffusion-controlled mechanism Smith and Ewart [39]	$k_e = 2\pi d_s N_A D_{w(i)} f_e$ f_e : Efficiency of radical entrance (taken equal to 1)
Radical exit/desorption from particles [39–41]	
Radical desorption rate per particle Smith and Ewart [39]	$R_{\text{des}} = k_{\text{des}}(v, t) \bar{n}(v, t)$ $k_{\text{des}} = \frac{ap'}{v} = \frac{6}{d} k_0$ with: $k_0 = k_{\text{des}0} + k_{\text{des}1} [CTA]_p$ [34] $k_{\text{des}0} = 1 \times 10^{-4} \text{ s}^{-1}$ $k_{\text{des}1} = 1.3 \times 10^{-6} \text{ m}^3 \text{ mol}^{-1} \text{ s}^{-1}$
Combining Friis & Nyhage [40] and Ugelstad & Hansen (1976) [41]	$P = \frac{k_0}{k_0 + k_p [M]_p}$ [40] $k_0 = \frac{12D_p D_w}{d^2(mD_p + D_w)}$ [41] $k_{\text{des}} = P(k_{fM} [M]_{p,am} + k_{fCTA} [CTA]_p)$ $m = \frac{[M]_w^{\text{eq}}}{[M]_p^{\text{eq}}}$ Assuming $D_p = D_w$
Particle size distribution and particle growth	
PSD: $f(v, t)$ (part m^{-3} of emulsion m^{-3} of polymer) is the particle density distribution	$\frac{\partial}{\partial t} f(v, t) = -\frac{\partial}{\partial v} [G(v, t) f(v, t)]$
The growth rate of unswollen particles ($\text{m}^3 \text{ s}^{-1}$)	$G(v, t) = \bar{n}(v, t) \frac{k_p [M]_p M_{w,m}}{N_A \rho_p}$
Average number of radicals per particle: pseudo-bulk model	
Radicals into particles	$\frac{\partial}{\partial t} \bar{n}(v, t) = \rho_e - k_{\text{des}}(v) \bar{n}(v, t) - 2c(v) \bar{n}(v, t)^2$
Radical termination	$c = \frac{k_{tp}}{N_A v}$
Radical entry	$\rho_e = k_e [R^*]_w$
Concentrations of monomer	
Concentration of monomer in amorphous polymer and water	$\frac{d[M]_p}{dt} = k_L a ([M]_p^{\text{eq}} - [M]_p) - \frac{V_e}{V_{p,am}} R_p$ $\frac{[M]_w}{[M]_w^{\text{eq}}} = \frac{[M]_p}{[M]_p^{\text{eq}}}$ The $k_L a$ values come from Equation 4 and Table 4 $V_{p,am} = (1 - \chi) V_p$ With $\chi = 0.5$, the volumetric crystallinity
The concentration of monomer in the gas phase	$[M]_g = \frac{P}{zRT}$
Compressibility factor for VDF	$Z = -0.0077P_r^3 + 0.117P_r^2 - 0.4831P_r + 1.1543$
Equation developed by Nelson and Obert [42]	$P_r = \frac{P}{P_c}$, with $P_c = 44.3 \text{ bar}$
Equilibrium concentration of monomer in amorphous polymer from Henry's law	$[M]_p^{\text{eq}} = H_{e,p} P_m$

Table 6. Model Parameters.

Parameter	Value
Decomposition rate coefficient k_d (s^{-1}) [34]	$4.56 \times 10^{16} \exp\left(\frac{-16860}{T}\right)$
Propagation rate coefficient k_p ($m^3 mol^{-1} s^{-1}$) [34]	$2.2 \times 10^6 \exp\left(\frac{-4539}{T}\right)$
Transfer to monomer rate coefficient k_{fm} ($m^3 mol^{-1} s^{-1}$) [34]	$1.2 \times 10^8 \exp\left(\frac{-9020}{T}\right)$
Transfer to CTA rate coefficient in the particles k_{fCTA} ($m^3 mol^{-1} s^{-1}$)	$1.1 \times 10^3 \exp\left(\frac{-4539}{T}\right)$
Termination in water rate coefficient k_{tw} ($m^3 mol^{-1} s^{-1}$) [43]	$\left(\frac{k_p}{0.14}\right)^2$
Termination in particles rate coefficient k_{tp} ($m^3 mol^{-1} s^{-1}$) – analog to styrene	$0.05 k_{tw}$
Henry coefficient at 80 °C $H_{e,p}$ ($mol Pa^{-1} m^{-3}$ am polymer) [25]	3.1×10^{-4}
Equilibrium concentration of monomer in water $[M]_w^{sat}$ ($mol m^{-3}$ at 83 °C and 85 bar) [34]	10^2
Monomer diffusion coefficient in water D_w ($m^2 s^{-1}$)	1.5×10^{-9}
Initiator efficiency f_I (-)	0.6

Initial condition of the model

As the model does not take into consideration the nucleation stage, seeded reactions are performed to generate the experimental results to be modelled. In this system, repressurizing seeds was found to be delicate and not reproducible, as some coagulation was observed. As an alternative, first several replicate semi-batch runs were performed to ensure that the experiments were reproducible during the nucleation period, even when changing the agitator type or speed. We estimated that the main nucleation phase is over after 40 minutes of polymerization, when comparing the number of particles obtained in 40 minutes and after 120 minutes of reaction. The polymerization rate profiles for the starting point data are shown in Figure 5. The results of the reaction used as initial condition are presented in Table 7. The reaction stopped at the end of the nucleation period was used as initial point for the model to simulate longer duration experiments (starting from 40 min until the end of the reaction).

The reactions performed with different setups and agitation speeds presented in the previous section were simulated to evaluate the robustness of the model.

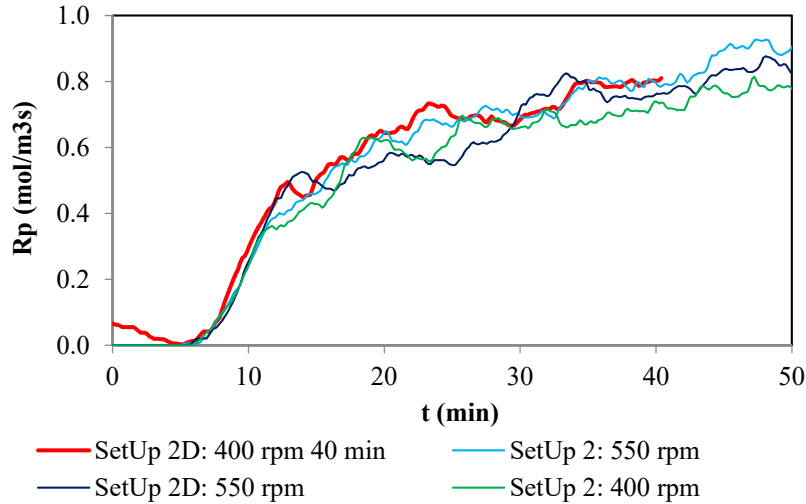


Figure 5: Polymerization rate for the first 40 minutes of semi-batch reactions performed with different setups and speeds.

Table 7: Results of semi-batch polymerization stopped at 40 minutes.

Time (min)	40
SC (%)	9.9
d_p (nm)	145
PdI	0.01
$N_p \times 10^{-19}$ (1/m³)	3.7
θ (%)	16.8
M_w (kDa)	310
PDI	3.12

Effect of mixing on the concentration of monomer in amorphous polymer

Figure 6 presents the model prediction of the monomer concentration in the amorphous polymer particles and time zero correspond to the 40 minutes of the initial condition reaction. As already mentioned, the equilibrium concentration of monomer calculated by Henry's Law is only affected by pressure and temperature, and is not influenced by the agitation type or speed. If the model does not take into consideration the mass transfer limitations, it is assumed that the concentration of monomer in the polymer particles is at equilibrium. It is possible to observe that the concentration of monomer in the particles is below the equilibrium value, especially for the lowest agitation speed. An increase in the agitation speed increases this concentration, and as observed from the reaction results, the monomer concentration curves at 550 rpm are virtually the same with the different setups. The results show that the use of a non-equilibrium model is essential when the agitation speed is low, but the results at 550 rpm are close to Henry's law.

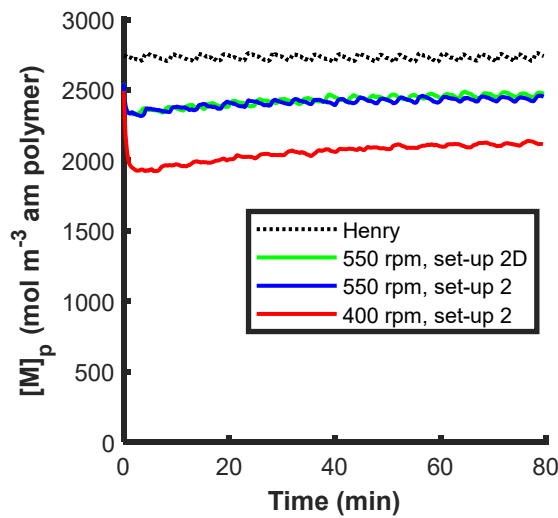
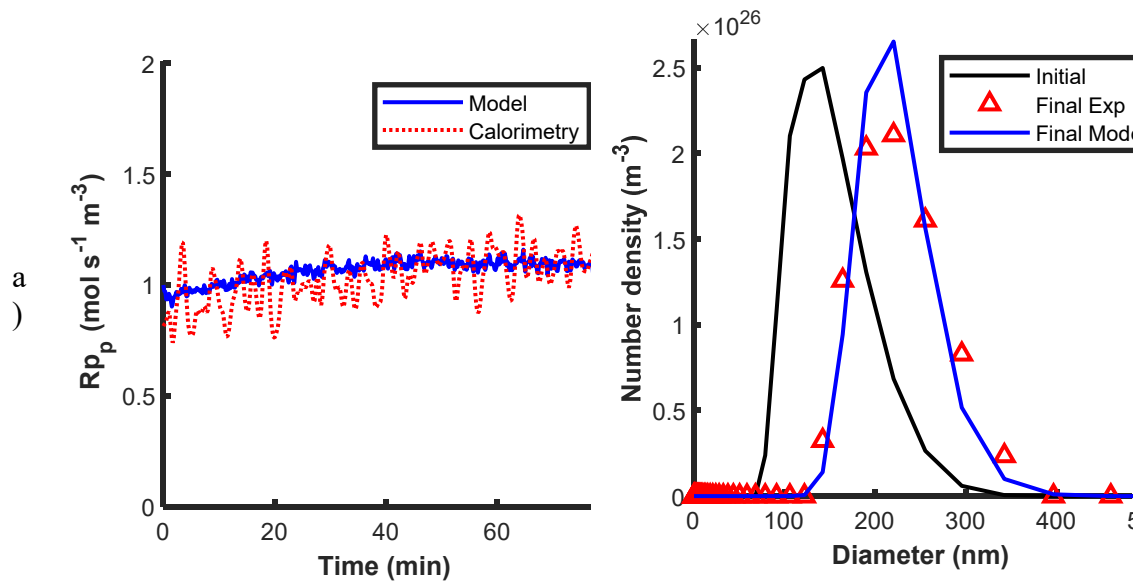


Figure 6: Prediction of the monomer concentration in amorphous polymer.

Influence of different models of the average number of radicals per particle

The impact of different models for the radical desorption rates are tested using Smith and Ewart [44] and a model combining the works of Friis and Nyhagen [40] and Ugelstad and Hansen [41]. The reaction performed at 550 rpm with the setup 2 is used to compare the models and the results are presented in Figure 7. The evolution of \bar{n} as a function of time is shown in Figure 8, and justifies the assumption of pseudo-bulk conditions as it is superior to 1 throughout the modelled period. It is possible to observe the general improvement in the particle size distribution and polymerization rate when using the Friis & Nyhagen (1973) [40] and Ugelstad & Hansen (1976) [41] models.



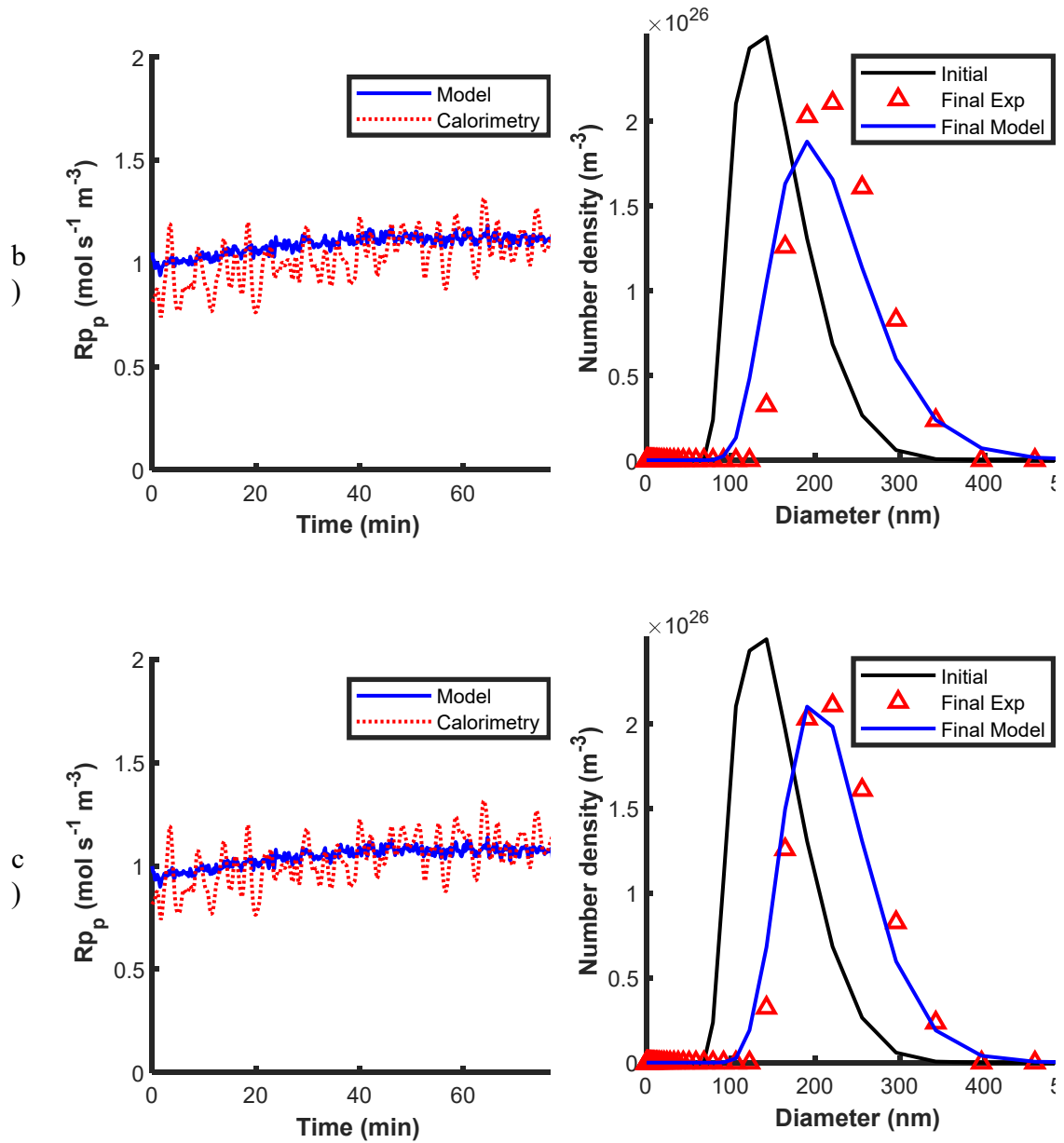


Figure 7: Influence of \bar{n} model a) Constant $\bar{n} = 1.6$, b) Using Smith & Ewart desorption model, and c) Using Friis & Nyhagen and Ugestald & Hansen radical desorption model (time 0 corresponds to the end of the nucleation period).

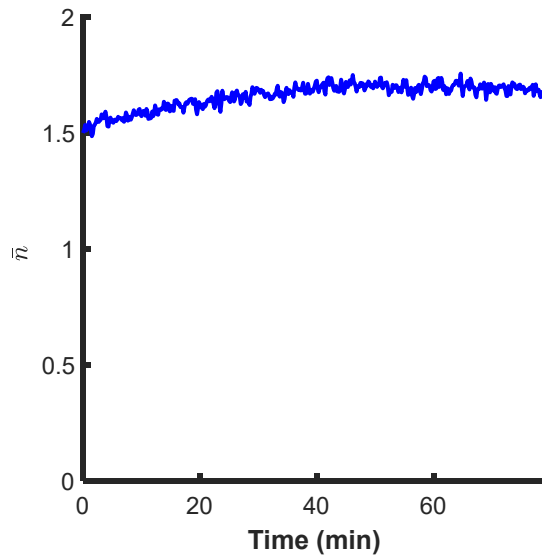


Figure 8: Variation of \bar{n} justifying the assumption of pseudo-bulk behaviour.

Effect of mixing on the reaction rate

Figure 9 shows that the model fits well the experimental data by calorimetry and that the polymerization rate using setup 2D is slightly higher than the one performed with setup 2. As the monomer concentration in the particles is lower for the agitation speed of 400 rpm, it was expected that the polymerization rate follows this behavior.

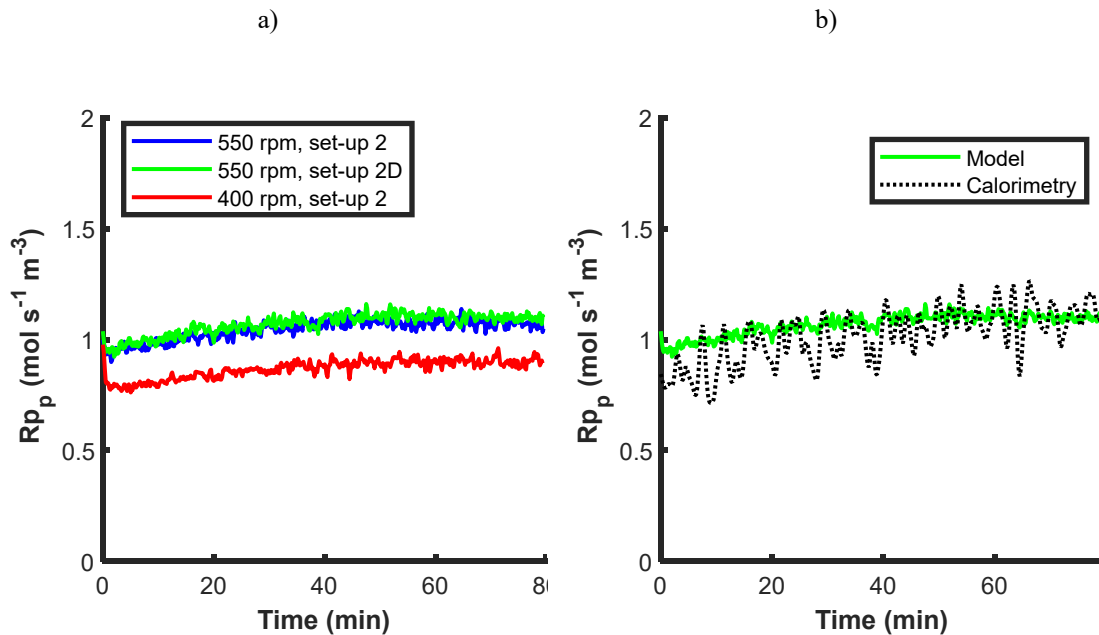


Figure 9: Polymerization rate a) from the model and b) compared to the experimental results from calorimetry (for setup 2D at 550 rpm)

Effect of mixing on the particle size distribution

Figure 10 shows the effect of mixing on the particle size distribution for the reactions performed with different setups and speeds. We can observe that the model fits the experimental data, and as only the particle growth is modelled, different polymerization

rates will have an impact on the final particle size distribution. As the polymerization rate at 550 rpm was virtually independent of the setup used, the final particle distributions of both setups are also similar. At 400 rpm the polymerization rate is slower, not leading to same growth of particles, which is reflected by the slightly smaller particles obtained.

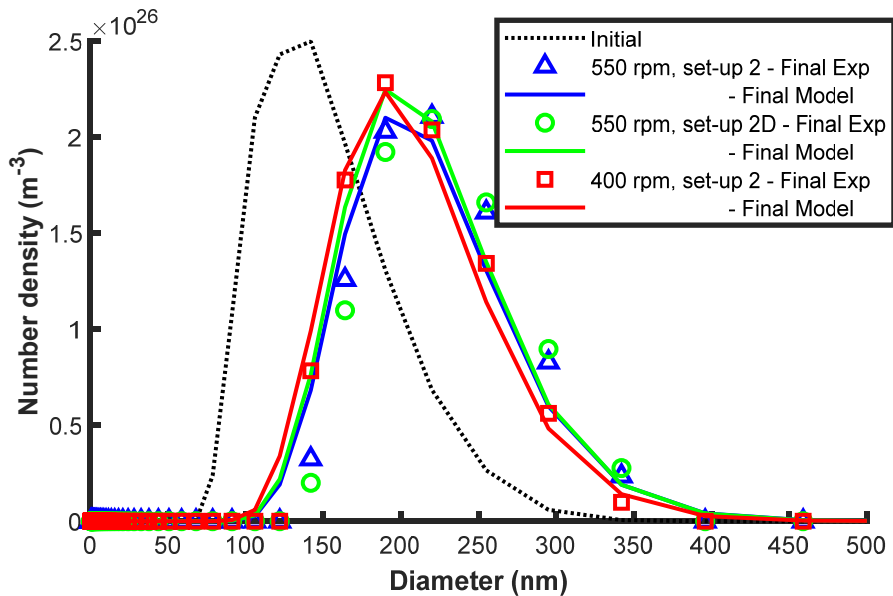


Figure 10: Initial (experimental) and final particle size distributions (experimental and by the model).

Importance of a $k_t a$ Model

The importance of a non-equilibrium model taking into account the mass transfer coefficient during the reaction is shown in Figure 11 and Figure 12. It can be seen that when a model is considering that the monomer concentration in the polymer particles is at thermodynamic equilibrium, there is an overestimation of the polymerization rate. The overestimation of the polymerization rate will also lead to slightly overestimation the size of particles.

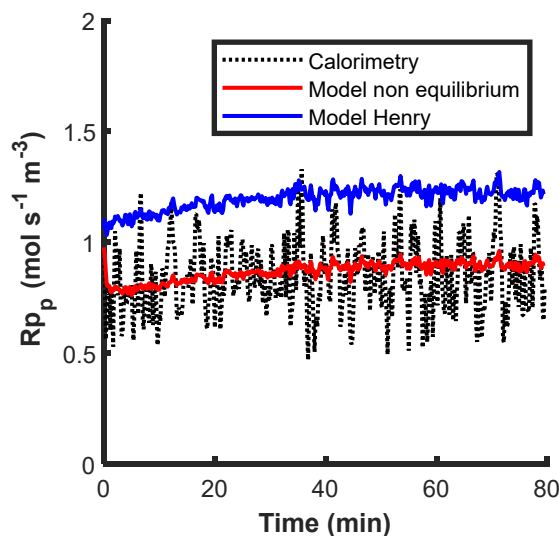


Figure 11: Polymerization rate by non-equilibrium and Henry models.

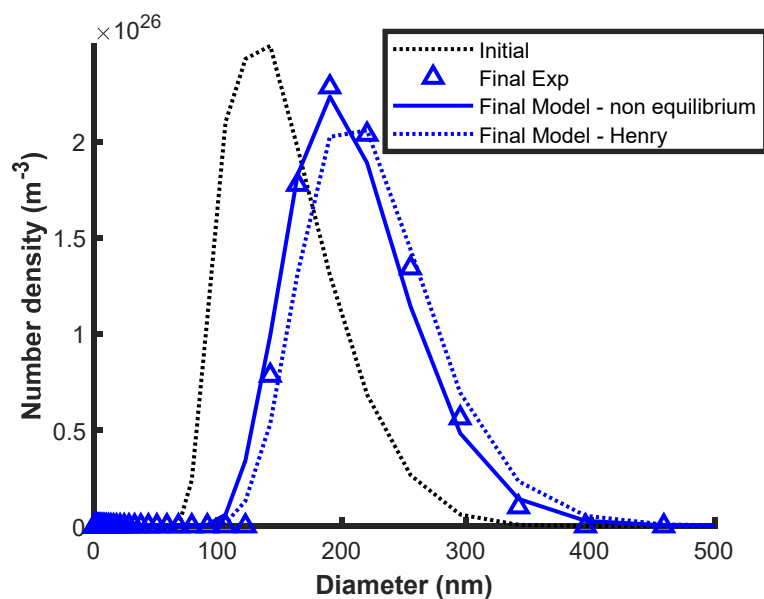


Figure 12: Initial and final particle size distributions for non-equilibrium and Henry models.

CONCLUSIONS

Experimental evidence of the importance of mass transfer in the emulsion polymerization of VDF has been presented, as well as the impact of changing the agitator.

A simplified model that does not take into account nucleation or coagulation allows us to account for the influence of the mass transfer resistances on the monomer concentration in the polymer particles. This model shows that at agitation rates of less than 550 rpm, the polymerization is limited by mass transfer from the entrained droplets. It is important to note that besides the type of impeller and agitation speed other parameters influence the $k_L a$, and so mass transfer, such as the viscosity of the latex (or solids content, particles size) and the level of latex in the reactor (e.g. vortex).

ACKNOWLEDGEMENTS

The authors thank Arkema for providing the monomer and surfactant used in this study and the ANR Clean-Poly project (ANR-18-CE06-0023) for financial support.

REFERENCES

- [1] J.C. Ramirez, J. Herrera-Ordóñez, H. Maldonado-Textle, Kinetics of the styrene emulsion polymerization above cmc. II. Agitation effect on molecular weight, *Polym. Bull.* 53 (2005) 333–337.
- [2] M.F. Kemmere, J. Meuldijk, A.A.H. Drinkenburg, A.L. German, Colloidal Stability of High-Solids Polystyrene and Polyvinyl Acetate Latices, *J. Appl. Polym. Sci.* 74 (1999) 1780–1791.
- [3] S.F. Roudsari, Experimental and CFD Investigation of the Mixing of MMA Emulsion Polymerization in a Stirred Tank Reactor, Ryerson University, 2015.
- [4] K. Arai, M. Arai, S. Iwasaki, S. Saito, Agitation effect on the rate of soapless emulsion polymerization of methyl methacrylate in water, *J. Polym. Sci. Part A Polym. Chem.* 19 (1981) 1203–1215.
- [5] M. Zubitur, J.M. Asua, Agitation effects in the semicontinuous emulsion polymerization of styrene and butyl acrylate, *J. Appl. Polym. Sci.* 80 (2001) 841–851. doi:10.1002/1097-4628(20010509)80:6<841::AID-APP1162>3.0.CO;2-4.
- [6] J. Hong, Effects of Agitation in Emulsion Polymerization - Kinetic and Mechanistic Study of Coagulum, Lehigh, 2008.
- [7] M. Nomura, M. Harada, W. Eguchi, S. Nagata, Effect of stirring on the emulsion polymerization of styrene, *J. Appl. Polym. Sci.* 16 (1972) 835–847. doi:10.1002/app.1972.070160403.
- [8] S.F. Roudsari, R. Dhib, F. Ein-Mozaffari, Using a Novel CFD Model to Assess the Effect of Mixing Parameters on Emulsion Polymerization, *Macromol. React. Eng.* 10 (2016) 108–122. doi:10.1002/mren.201500019.
- [9] S.F. Roudsari, R. Dhib, F. Ein-Mozaffari, Mixing Effect on Emulsion Polymerization in a Batch Reactor, *Polym. Eng. Sci.* (2015) 945–956. doi:10.1002/pen.
- [10] S. Oprea, T. Dodita, Influence of agitation during emulsion polymerization of acrylic-styrene latexes on end product properties, *Prog. Org. Coatings.* 42 (2001) 194–201.
- [11] C.-S. Chern, C.-H. Lin, Semi-batch Surfactant-Free Emulsion Polymerization of Butyl Acrylate, *Polym. J.* 24 (1995) 1094–1103.
- [12] J. Mendoza, J.C. De La Cal, J.M. Asua, Kinetics of the styrene emulsion polymerization using n-dodecyl mercaptan as chain transfer agent, *J. Polym. Sci. Part A Polym. Chem.* 38 (2000) 4490–4505.
- [13] C. Kiparissides, J.F. MacGregor, A.E. Hamielec, Continuous Emulsion Polymerization of Vinyl Acetate. Part I: Experimental Studies, *Can. J. Chem. Eng.* 58 (1980) 48–55.
- [14] S. Krishnan, A. Klein, M.S. El-Aasser, E.D. Sudol, Effects of agitation on oxygen inhibition, particle nucleation, reaction rates, and molecular weights in emulsion polymerization of n-butyl methacrylate, *Ind. Eng. Chem. Res.* 43 (2004) 6331–6342. doi:10.1021/ie049796r.
- [15] B.G. Clarkson, An investigation into the Effect of Agitation on Polymer Properties in Emulsion Polymerization, Imperial College, University of London, 1988.

- [16] P. Bataille, J.F. Dalpé, F. Dubuc, L. Lamoureux, The Effect of Agitation on the Conversion of Vinyl Acetate Emulsion Polymerization, *J. Appl. Polym. Sci.* 39 (1990) 1815–1820.
- [17] P.J. Scott, A. Penlidis, G.L. Rempel, Reactor Emulsion Design Considerations for Gas-Liquid Emulsion Polymerizations: the Ethylene-Vinyl Acetate Example, *Chem. Eng. S.* 49 (1994) 1573–1583.
- [18] I. Poljanšek, E. Fabjan, D. Kukanja, Emulsion copolymerization of vinyl acetate-ethylene in high pressure reactor-characterized by inline FTIR spectroscopy, *Prog. Org. Coatings.* 76 (2013) 1798–1804.
- [19] H.S. Mobarakeh, M.R.R. Daronkola, Effect of different parameters in emulsion copolymerization of vinyl acetate-ethylene in 7.5 liter high pressure reactor, *Iran. Polym. J.* 14 (2005) 579–587.
- [20] Y.H. Choi, W.K. Lee, Effects of agitation in emulsion polymerization of vinyl acetate, ethylene, and N-methylol acrylamide, *J. Ind. Eng. Chem.* 16 (2010) 431–436. doi:10.1016/j.jiec.2010.01.042.
- [21] Tetrafluoroethylene, *Cameo Chem. Database.* (1999). cameochemicals.noaa.gov/chris/TFE.pdf (accessed April 18, 2023).
- [22] C.U. Kim, J.M. Lee, S.K. Ihm, Emulsion polymerization of tetrafluoroethylene: effects of reaction conditions on the polymerization rate and polymer molecular weight, *J. Appl. Polym. Sci.* 73 (1999) 777–793. doi:10.1002/(SICI)1097-4628(19990801)73:5<777::AID-APP18>3.0.CO;2-C.
- [23] T. Hjertberg, Polymerization of vinyl chloride at reduced monomer accessibility. IV. The effect of diffusion control on polymerization rate, molecular weight, and thermal stability, *J. Appl. Polym. Sci.* 36 (1988) 129–140.
- [24] A.C.M. Ecoscia, N. Sheibat-Othman, T.F.L. McKenna, Emulsion polymerization of vinylidene fluoride: Effects of mixing and reaction conditions on the initial rate of polymerization, *Can. J. Chem. Eng.* 100 (2022) 654–665. doi:10.1002/cjce.24145.
- [25] M. Apostolo, V. Arcella, G. Storti, M. Morbidelli, Kinetics of the Emulsion Polymerization of Vinylidene Fluoride and Hexafluoropropylene, *Macromolecules.* 32 (1999) 989–1003. doi:10.1021/ma980683r.
- [26] H.Z. Liu, M.H. Wang, Z.F. Wang, J.M. Bian, Kinetics of waterborne fluoropolymers prepared by one-step semi-continuous emulsion polymerization of chlorotrifluoroethylene, vinyl acetate, butyl acrylate and Veova 10, in: *IOP Conf. Series: Materials Science and Engineering*, 2018.
- [27] E.L. Paul, V.A. Atiemo-Obeng, S.M. Kresta, eds., *Handbook of Industrial Mixing: Science and Practice*, John Wiley & Sons, Ltd, New Jersey, 2004.
- [28] A.C. Mendez Ecoscia, N. Sheibat-Othman, T.F.L. McKenna, Reaction engineering of the emulsion homopolymerization of vinylidene fluoride: Progress and challenges, *Can. J. Chem. Eng.* (2018) 1–10. doi:10.1002/cjce.23308.
- [29] R. V. Chaudhari, R. V. Gholap, G. Emig, H. Hofmann, Gas-liquid mass transfer in “dead-end” autoclave reactors, *Can. J. Chem. Eng.* 65 (1987) 744–751. doi:10.1002/cjce.5450650506.
- [30] T. Moucha, V. Linek, E. Prokopová, Gas hold-up, mixing time and gas-liquid

- volumetric mass transfer coefficient of various multiple-impeller configurations: Rushton turbine, pitched blade and techmix impeller and their combinations, *Chem. Eng. Sci.* 58 (2003) 1839–1846.
- [31] R. Sardeing, J. Aubin, C. Xuereb, Gas-Liquid Mass Transfer. A Comparison of Down- and Up-pumping Axial Flow Impellers with Radial Impellers, *Trans IChemE Part A.* 82 (2004) 1589–1596.
- [32] M. Teramoto, S. Tai, K. Nishii, H. Teranishi, Effects of pressure on liquid-phase mass transfer coefficients, *Chem. Eng. J.* 8 (1974) 223–226.
- [33] P. Pladis, A.H. Alexopoulos, J. Bousquet, C. Kiparissides, Modelling of vinylidene fluoride emulsion polymerization, *Comput. Aided Chem. Eng.* 20 (2005) 319–324. doi:10.1016/S1570-7946(05)80175-0.
- [34] P. Pladis, A.H. Alexopoulos, C. Kiparissides, Mathematical Modeling and Simulation of Vinylidene Fluoride Emulsion Polymerization, *Ind. Eng. Chem. Res.* 53 (2014) 7352–7364. doi:10.1021/ie403548m.
- [35] R.G. Gilbert, *Emulsion Polymerization. A Mechanistic Approach*, Academic Press Limited, London, 1995.
- [36] J.M. Asua, ed., *Polymeric Dispersions: Principles and Applications*, 1st ed., Springer Science+Business Media Dordrecht, 1997.
- [37] J.M. Asua, ed., *Polymer Reaction Engineering*, 1st Ed., Blackwell, Oxford, 2007.
- [38] E.M. Coen, R.G. Gilbert, B.R. Morrison, H. Leube, S. Peach, Modelling particle size distributions and secondary particle formation in emulsion polymerisation, *Polymer (Guildf)*. 39 (1998) 7099–7112. doi:10.1016/S0032-3861(98)00255-9.
- [39] W. V. Smith, R.H. Ewart, Kinetics of Emulsion Polymerization, *J. Chem. Phys.* 16 (1948) 592–599. doi:10.1002/app.1965.070090410.
- [40] N. Friis, L. Nyhagen, A kinetic study of the emulsion polymerization of vinyl acetate, *J. Appl. Polym. Sci.* 17 (1973) 2311–2327. doi:10.1002/app.1973.070170802.
- [41] J. Ugelstad, F.K. Hansen, Kinetics and Mechanism of Emulsion Polymerization, *Rubber Chem. Technol.* 50 (1976) 536–640.
- [42] R.C. Reid, J.M. Prausnitz, B.E. Poling, *The Properties of Gases and Liquids*, Fourth, McGraw-Hill Inc., New York, 1987.
- [43] B. Ameduri, From Vinylidene Fluoride (VDF) to the Applications of VDF-Containing Polymers and Copolymers: Recent Developments and Future Trends, *Chem. Rev.* 109 (2009) 6632–6686. doi:10.1002/chin.201017230.
- [44] W. V. Smith, R.H. Ewart, Kinetics of emulsion polymerization, *J. Chem. Phys.* 16 (1948) 592–599. doi:10.1063/1.1746951.